ANALYSIS OF INJECTION AND RECOVERY SCHEMES FOR A MULTI-TURN ERL BASED LIGHT SOURCE*

Y. Petenev[#], T. Atkinson, A.V. Bondarenko, A.N. Matveenko
Helmholtz-Zentrum Berlin für Materialien und Energie GmbH, Germany

Abstract

A multi-turn energy recovery linac -based light source is under discussion. Using the superconducting Linac technology, the Femto-Science-Factory(FSF) will provide its users with ultra-bright photon beams of angstrom wavelength. The FSF is intended to be a multi-user facility and offer a variety of operation modes. The driver of the facility is a 6 GeV multiturn energy recovery linac with a split linac.

In this paper we discuss designs of the optic in the linac and compare different schemes of beam acceleration: a direct injection scheme with acceleration in a 6 GeV linac, a two-stage injection with acceleration in a 6 GeV linac, and a multi-turn (3-turn) scheme with a two-stage injection and two main 1 GeV linacs. The key characteristic of comparison is the beam breakup (BBU) instability threshold current.

INTRODUCTION

Our group at Helmholtz Zentrum Berlin is designing a new future multi-turn Energy Recovery Linac (ERL) based light source (LS) with 6 GeV maximum energy of electron beam. This future facility is named Femto-Science Factory (FSF) [1].

One potential weakness of the ERLs is transverse beam breakup (BBU) instability, which may severely limit a beam current. If an electron bunch passes through an accelerating cavity it interacts with dipole modes (e.g. TM_{110}) in the cavity. First, it exchanges energy with the mode; second, it is deflected by the electro-magnetic field of the mode. After recirculation the deflected bunch interacts with the same mode in the cavity again which constitutes the feedback. If net energy transfer from the beam to the mode is larger than energy loss due to the mode damping the beam becomes unstable.

The actuality of this problem was recognized in early experiments with the recirculating SRF accelerators at Stanford [2] and Illinois [3], where threshold current of this instability was occurring at few microamperes of the average beam current. In the works of Rand and Smith in [4] dipole high order modes were identified as a driver of this instability. In late of the 80's the detailed theoretical model and simulation programs had been developed [5, 6]. Nowadays the interest to this problem was renewed. The requirements for more detailed theory and simulation programs [7-9] are given by the needs of high current (~100 mA) ERLs.

In this document we compare different schemes of acceleration for FSF: a direct injection scheme with acceleration in a 6 GeV linac, a two-stage injection with acceleration in a 6 GeV linac, and a multi-turn (3-turn) scheme with a two-stage injection and two main linacs.

DIRECT INJECTION SCHEME

In this part we discuss the simplest scheme of an ERL based LS. In this scheme the beam after an injector section goes directly to the main linac (see Fig. 1), where it accelerated up to 6 GeV and used for the experiments, and after the recirculation turn it arrives to the linac and decelerated there. After the deceleration the beam goes to the dump.
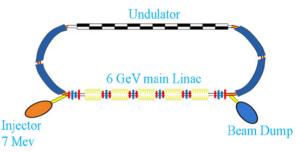

Figure 1: Direct injection scheme.

The linac is planned to be based on the BERLinPro[12] 7-cell cavities. To reach 6 GeV in the Linac we took 464 cavities with an accelerating gradient G about 16 MeV/m and distributed them over 58 cryomodules. The cryomodule is schematically presented in Fig. 2, where λ~0.231 m is the wavelength of the accelerating mode.
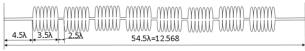

Figure 2: The scheme of FSF cryomodule.

Triplets of quadrupoles are planned to be in between the cryomodules in the linac and were optimized in such a way that the BBU instability will develop similarly for all the cavities in the linac. In this case the highest threshold current might be achieved. The threshold current for the transverse beam breakup may be estimated for the case of a single cavity and single mode for a multipass ERL in the form as [9]:

$$I_{th} \approx I_0 \frac{\lambdabar^2}{Q_a L_{eff} \sqrt{\sum_{m=1}^{2N-1} \sum_{n=m+1}^{2N} \frac{\beta_m \beta_n}{\gamma_m \gamma_n}}}, \qquad (1)$$

where I_0- Alfven current, Q_a is the quality factor of HOM, $\lambdabar = \lambda/2\pi$, λ is the wavelength corresponding to the resonant frequency of the TM_{110} mode, γ_m is the Lorentz factor at the m-th pass through the cavity, β_m – is the Twiss parameter, L_{eff} – is the effective length of the cavity, N is the number of passes during acceleration.

One can see from (1) that the threshold current is higher when the square root in the denominator is minimized. We will use this eq. to find the best optic solution assuming the HOM nature is predictable. But however there could be some unique set of the HOMs parameters when there will exist a better optic solution. The most dangerous for the BBU stability are the cavities where the beam has the lower energies. Therefore the initial Twiss parameters before the linac were optimized to minimize the beta functions in the first cryomodule. In this cryomodule the energy is changed from 7 to 110 MeV. And an RF focusing, which was described in [10] still affect the beam in the first cavities.

To estimate the optimum values of the initial Twiss parameters we used the cavity model given by [10]:

$$\begin{pmatrix} \cos(\alpha) - \sqrt{2}\sin(\alpha) & \dfrac{\sqrt{8}\gamma_0 L \sin(\alpha)}{(\gamma_1 - \gamma_0)} \\ -\dfrac{3}{\sqrt{8}}\dfrac{(\gamma_1 - \gamma_0)\sin(\alpha)}{L\gamma_1} & \left(\cos(\alpha) + \sqrt{2}\sin(\alpha)\right)\dfrac{\gamma_0}{\gamma_1} \end{pmatrix}, (2)$$

where $\alpha = \dfrac{1}{\sqrt{8}}\ln\left(\gamma_1 / \gamma_0\right)$, $\gamma_{1(0)}$ is the final(initial) normalized energy of the particle, L – the length of the cavity (or cryomodule). Also we assume that there are symmetrical β-functions on acceleration and deceleration in the linac and that the cryomodule is one long cavity with an effective gradient given by:

$$G_{eff} = G\frac{8L_{cav}}{L_{cryo}}, \qquad (3)$$

where L_{cav} is the length of the cavity and L_{cryo} the length of the cryomodule.

We can transfer the beta function through the 1st cryomodule as:

$$\beta_1 = \frac{\gamma_1}{\gamma_0}(\beta_0 m_{11}^2 - 2\alpha_0 m_{11}m_{12} + \frac{1+\alpha_0^2}{\beta_0}m_{12}^2), (4)$$

where m_{11} and m_{12} - the coefficients of the transfer matrix of the cryomodule given by (2). Now we just have to minimize β_1 in (4) for the initial Twiss parameter α_0, what gives:

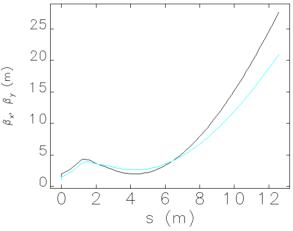$$\alpha_0 = \frac{m_{11}}{m_{12}}\beta_0. \qquad (5)$$

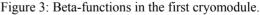We also want to keep constant the value of β/γ:

$$\frac{\beta_0}{\gamma_0} = \frac{\beta_1}{\gamma_1}. \qquad (6)$$

The solution is given by:

$$\begin{cases} \beta_0 = m_{12} \sim 2\,m \\ \alpha_0 = m_{11} \sim -0.61 \\ \beta_1 = \dfrac{\gamma_1}{\gamma_0}m_{12} \sim 31\,m \end{cases} \qquad (7)$$

Modelling in the Elegant [11] program shows similar results but of course our model is not ideal. Because we assumed one long cavity instead of 8 short with drifts in between. Therefore the initial Twiss parameters of the beam were adjusted to get the smaller value of the β_1. In Fig. 3 we show the difference in optic given by the theoretic results from (7) and after an optimization in Elegant. The black curve (β_x) shows the dependence of the beta-function for the theoretical and the blue (β_y) one for the initial parameters optimized by elegant.
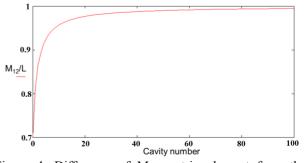

Figure 3: Beta-functions in the first cryomodule.

Figure 4: Difference of M_{12} matrix element from the length of the cavity for different cavities.

Later on the higher energies the RF focusing can be neglected. Therefore, we can use the model of cavity as a free drift but with acceleration. In Fig. 4 we show the dependence of (M_{12}/L) for different cavities. On the x axis the number of the cavity is shown and on the y axis one can see how the matrix element which is responsible for RF focusing differs from the length of the cavity L. And the results show that they quite fast reach each other and for the last cavity of the first cryomodule this coefficient is about 0.95.

So our goal is to keep constant the values of β/γ, the preferable theoretically for the BBU stability optics should look then like it is shown in Fig. 5.
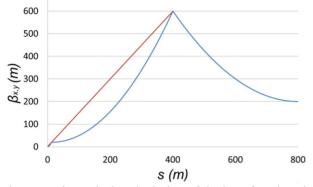

Figure 5: Theoretical optic design of the beta-functions in the main linac for the direct injection scheme.

The red line shows the values with a constant $\beta/\gamma \sim 0.1$ m, and the values below this line will give a higher threshold current. Optics calculated in Elegant using this pattern is presented in Fig. 6.
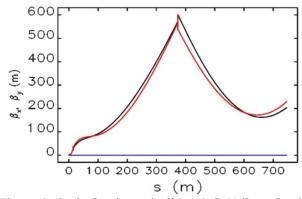

Figure 6: Optic for the main linac 6 GeV linac for the direct injection scheme.

It should be noted that we used only 5 triplets (between first and second, between 8th and 9th cryomodules and in the middle of the linac, and as we said optics has a mirror symmetry therefore there are two more triplets one the second half of the linac) and the length of the linac is then about 750 m.

The main disadvantage of this scheme is the high ratio between the injection energy E_{in}=7 MeV and the final energy E_{fin}=6 GeV: $E_{in}/E_{fin} \sim 850$. What complicates the transverse focusing in the main linac, because the triplets which focus a beam at the beginning of the linac will not

affect the beam at the same position on the deceleration phase. For a given optics in Fig. 6 one can estimate the value of the threshold current using: $I_{th} = \frac{10^{-6}}{4\pi}\frac{E}{\beta} \sim 400\ mA$ for the middle point of the linac. For the estimations we took a mode with $(R/Q)_d \cdot Q_d$=6·10^5 Ω, ω=2π·2·10^9 Hz.

TWO STAGE INJECTION SCHEME

In this part we discuss an improved scheme of ERL based light source, which is presented in Fig. 7.
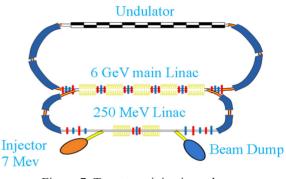

Figure 7: Two stage injection scheme.

The main improvement is that now a beam after an injector goes to a short linac, where it is accelerated up to 250 MeV, then it passes the first arc and comes to the main linac where it accelerated up to 6 GeV. After that it might be used as a light source. And after the beam was used it goes back on the deceleration phase. Our goal again will be to find the optimum optic solution for the beam break up stability in the both linacs. But first let us discuss the stability in the preinjection linac.

Preinjector

For the preinjection linac we suggest to use two cryomodules with a triplet of quadrupole magnets in between. To find the optimum initial twiss conditions we will use the same approach as in the chapter about direct injection scheme. The role of the triplet is to change the sign of the Twiss parameter α of the beam. Let us find the initial injection Twiss parameters to have the equal threshold currents for the entrance and for the middle of the linac.

The beta-function through the 1st cryomodule transferred again by (4).

As we already said the role of the triplet is to change the sign of alpha, therefore we assume that at the entrance to the second cryomodule a beam will have β_1 and $-\alpha_1$. So the beta function at the end of the linac might be found as:

$$\beta_2 = \frac{\gamma_2}{\gamma_1}(\beta_1 t_{11}^2 + 2\alpha_1 t_{11}t_{12} + \frac{1+\alpha_1^2}{\beta_1}t_{12}^2). \quad (8)$$

where t_{11} and t_{12} are the transport elements of the second cryomodule. The minimum of the β_2 is given, when

$$\alpha_1 = -\frac{\beta_1}{t_{12}} t_{11}, \qquad (9)$$

which gives

$$\beta_2 = \frac{\gamma_2}{\gamma_1} \frac{t_{12}^2}{\beta_1}. \qquad (10)$$

Now we can proceed with an equation which gives the same threshold currents for the middle and the beginning (end) of the linac using (1):

$$\sqrt{\frac{\beta_0 \beta_2}{\gamma_0 \gamma_2}} = \frac{\beta_1}{\gamma_1}. \qquad (11)$$

Now we can find the initial beta-function:

$$\beta_0 = \frac{\gamma_0}{\gamma_1} \frac{\beta_1^3}{t_{12}^2}. \qquad (12)$$

And from Eq. 4 we get:

$$\beta_1 = \frac{m_{11}^2 \beta_1^3}{t_{12}^2} - 2 \frac{\alpha_0 m_{11} m_{12} \gamma_1}{\gamma_0} + \frac{1+\alpha_0^2}{\beta_1^3} t_{12}^2 m_{12}^2. \quad (13)$$

After the minimization over α_0 one can find the initial Twiss parameters:

$$\beta_0 = \sqrt{\frac{\gamma_1}{\gamma_0} \frac{m_{12}^3}{t_{12}}}, \quad \alpha_0 = m_{11} \sqrt{\frac{\gamma_1}{\gamma_0} \frac{m_{12}}{t_{12}}}. \qquad (14)$$

Using Elegant program we can find the matrix elements of the cryomodules: $m_{11} = -0.835$, $m_{12} = 1.62$ m. and $t_{12} = 7.261$ m. And finally we get the initial parameters: $\alpha_0 = -1.421$ and $\beta_0 = 2.757$ m. As we already said the role of the triplet of quadrupole magnets is to change the sign of the alpha-function. It should be noted
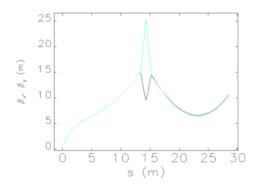

Figure 8: Optics design of the preinjection linac.

that the initial parameters we found there are located at the entrance to the cavity but not to the cryomodule (where it is about 1 m of a free drift Fig. 2), therefore we should send it back. The final optic is presented in Fig. 8.

The value of the threshold current for the same mode as in the part about direct injection scheme is $I_{th} = 1.64$ A. As we said before our goal was to have the same values of the threshold currents for all cavities in the linac. But in our model we assumed the same values for the first and the last cavity of the cryomodule in fact we got it the same but the value in the middle of cryomodule is higher (one can see this already from the Fig. 8) - about 2.5 A. In the next part we discuss the optics in the main Linac.

Main Linac

The main difference for the optic design between two schemes with direct injection and with a preinjector is that in the scheme with two stage injection the initial energy in the main linac is 250 MeV instead of 7 in the scheme with a direct injection. Therefore this strongly improves the optics. Because the quadrupole magnets which focus the beam on the low energies (>250 MeV) will also focus the beam on the high energies (<6 GeV).

On such high energies an RF focusing can be neglected and the cavity is like a free drift with acceleration. Therefore we calculate the optic in the following way: for the first half of the linac we adjust the triplets between the cryomodules in such a way that the beam will go like in a free drift with initial/final beta-functions about the length of the cryomodule (Fig. 9). The second part we assume to be symmetrical with the same optics on the deceleration, which is given from right to left in Fig. 9.
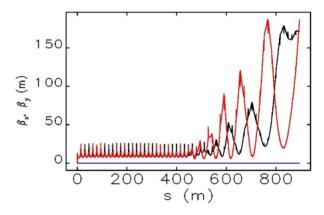

Figure 9: Two stage injection scheme.

For the first/last cavities estimations give the threshold current about 4 A and about 35 A for the middle of the linac for the same mode parameters as we used before.

Scalable scheme of FSF

In this part we present an upgrade of the acceleration scheme of FSF which was presented in [13]. In this scheme the acceleration in the preinjection linac and in two main linacs is assumed to be scalable. The injection energy is assumed to be $E_0 = 10$ MeV. The final energy of

a beam E_{fin} = 6 GeV, and E_{linac} = 960 MeV and E_{preinj} = 230 MeV are the energy gains in the main linacs and in

Optic for the 3 passes through the first and the second main linacs is presented in Figs. 11, 12.
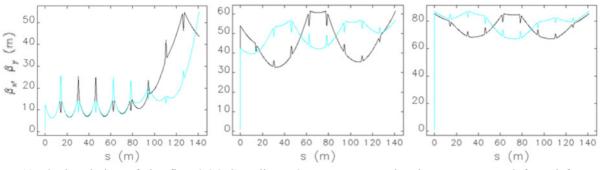

Figure 11: Optics design of the first 0.96 GeV linac. 3 passes on acceleration are presented from left to right correspondingly.
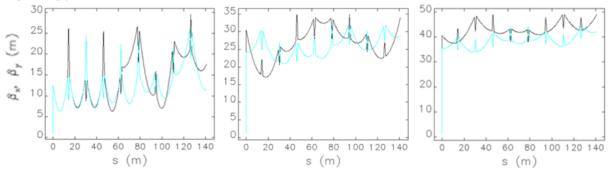

Figure 12: Optics design of the second 0.96 GeV linac. 3 passes on acceleration are presented from left to right correspondingly.

the preinjection linac correspondingly. So our main scheme of FSF is now looks like it presented in Fig. 10.
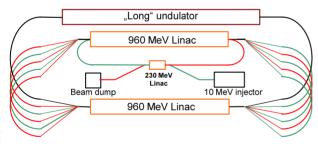

Figure 10: New scheme of a scalable FSF.

This change for the scalable facility was made because of the spreader design. A design of the spreader for 6 arcs is quite complicated and if the energy is changed somewhere due to unforeseen circumstances we could change field gradients of cavities in a proportional way to use the same spreader, therefore we would like to keep constant the deviations of the energies on different passes through the spreader. But it should be noted that accelerating gradients are different in the preinjector and in the main linacs.

Optic in the preinjection linac was optimized in the same way as it was described earlier in the preinjector subsection and it is similar to the Fig. 8.

The strengths of the quadrupoles were optimized to have the minimum of the beta functions on the 1-st pass.

In both linacs the optic is assumed to have mirror symmetry at the middle of the 5-th cryomodule. Optic for deceleration is then shown from right to left in Figs. 11, 12.

The threshold currents for this optic solution can be estimated using the following equation (which is a combination of Eq. 1 and [8]):

$$I_{th} = \frac{2mc^3}{e\omega\left(\frac{R}{Q}\right)_d Q_d} \frac{1}{\sqrt{\sum\limits_{m=1}^{5}\sum\limits_{n=m+1}^{6}\frac{\beta_m\beta_n}{\gamma_m\gamma_n}}} \qquad (15)$$

and for a mode which we always used before one could get for the beginning of the first linac I_{th} = 0.73 A and for the second I_{th} = 2.34 A, when for the preinjector it is about 1.14 A. What means the instability should develop in the first main linac.

CONCLUSION

We summarize the results of the threshold currents for different schemes in Table 1.

Table 1: Estimations of the threshold currents

Scheme	I_{th}, A
Direct injection	~0.4
Two stage injection	~1.64
Scalable FSF	~0.73

As one can see from the Table 1 from all 3 schemes the highest threshold current is given for the scheme with two stage injection and one turn. For the scheme of FSF the threshold current is about factor of 2 lower but it has a 3 times shorter main linac what makes it cheaper and smaller.

It should be noted that the values in table 1 are just the estimations of the threshold currents. These estimations were made assuming that it is only one mode in a cavity. In principle this is the comparison of the square roots in the denominator of Eq. 1 for the different cavities and different injection schemes. Therefore such problems like coupling and overlapping of the different modes are not taken into account. These problems will decrease the threshold current and, therefore, should be taken into account later.

REFERENCES

[1] Y. Petenev et al., "Feasibility Study of an ERL-Based GeV scale Multi-turn Light Source", IPAC2012, New Orleans, USA.

[2] Claude M. Lyneis, Michael S. McAshan, Roy E. Rand, H. Alan Schwettman, Todd I. Smith and John P. Turneaure, The Stanford Superconducting Recyclotron, IEEE Transactions on Nuclear Science, Vol. NS-26, No. 3, June 1979.

[3] P.Axel, L.S.Cardman, H.D.Graef, A.O.Hanson, R.A.Hoffswell, D.Jamnik, D.C.Sutton, R.H.Taylor, and L.M.Young, Operating Experience with MUSL-2, IEEE Transactions on Nuclear Science, Vol. NS-26, No. 3, June 1979.

[4] R.E. Rand and T.I. Smith, Beam optical control of beam breakup in a recirculating electron accelerator, Particle accelerators, Vol. 11, pp. 1-13 (1980).

[5] J.J. Bisognano, R.L. Gluckstern, in Proceedings of the 1987 Particle Accelerator Conference, Washington, DC (IEEE Catalog No. 87CH2387-9), pp. 1078-1080.

[6] G.A. Krafft, J.J. Bisognano, in Proceedings of the 1987 Particle Accelerator Conference, Washington, DC (IEEE Catalog No. 87CH2387-9), pp. 1356-1358.

[7] G.H. Hoffstaetter, I.V. Bazarov, „Beam-breakup instability theory for the energy recovery linacs", Phys. Rev. ST AB 7, 054401 (2004).

[8] E. Pozdeyev, et al., "Multipass beam breakup in energy recovery linacs", NIM A 557 (2006) 176-188.

[9] N.A. Vinokurov et al., Proc. of SPIE Vol. 2988, p. 221 (1997).

[10] J. Rosenzweig, L. Serafini. "Transverse particle motion in radio-frequency linear accelerators". Phys. Rev., E49 (1994), p. 1601.

[11] M. Borland, "Elegant: A Flexible SDDS-Compliant Code for Accelerator Simulation," APS LS-287, 2000.

[12] A.N. Matveenko, et al., "Status of the B*ERL*inPro optics design", Proc. of IPAC'11, pp.1500-1502.

[13] Y. Petenev et al., "Linac optics design for multi-turn ERL light source", LINAC2012, Tel Aviv, Israel.